A CAPABILITY MODEL FOR PASSIVE SPHERES AT HIGH ALTITUDES

By Forrest L. Staffanson and R. Gary Phibbs

University of Utah

INTRODUCTION

The motion of a sphere free falling in the high atmosphere deviates from gravitational acceleration according to the drag expression

$$a_V - g_V = a_D = \frac{\rho V^2 C_D A}{2m}$$

where a_V and g_V are the inertial and gravitational acceleration components along the trajectory. (Symbols are defined in the appendix.) Atmospheric density can be deduced from the motion according to

$$\rho = \frac{2m}{C_D A} \frac{a_V - g_V}{V^2}$$

Uncertainty in the result depends on uncertainty in the measured trajectory quantities, assumed drag coefficient, gravitational acceleration, and sphere constants. By assuming random independence, these uncertainties are related as follows:

$$\left(\frac{\delta \rho}{\rho}\right)^2 = \left(\frac{\delta a_V}{a_D}\right)^2 + \left(2\frac{\delta V}{V}\right)^2 + \left(\frac{\delta C_D A}{C_D A}\right)^2 + \left(\frac{\delta g_V}{a_D}\right)^2 + \left(\frac{\delta m}{m}\right)^2$$

Atmospheric temperature can be calculated from the deduced density profile within the validity of the hydrostatic equation and equation of state according to

$$T = \frac{M_W}{\rho}\left[\frac{\rho_0 T_0}{(M_W)_0} - \frac{1}{R^*}\sum_i (\rho g \, \Delta z)_i\right]$$

Uncertainty in the initial value T_0 and mean molecular weight, as well as in the aforementioned quantities, produce uncertainty in the calculated temperature.

$$\left(\frac{\delta T}{T}\right)_k^2 = \left(\frac{\delta \rho}{\rho}\right)_k^2 + \left(\frac{\delta M_W}{M_W}\right)_k^2 + \left(\frac{M_W}{\rho T}\right)_k^2 \left\{\left(\frac{T_0}{(M_W)_0}\delta \rho_0\right)^2 + \left(\frac{\rho_0}{(M_W)_0}\delta T_0\right)^2 + \left(\rho_0 T_0 \frac{\delta(M_W)_0}{(M_W)_0^2}\right)^2 \right.$$

$$\left. + \left(\frac{1}{R^*}\right)_k^2 \left[\sum_i^k \left[\left(\frac{\delta \rho}{\rho}\right)_i^2 + \left(\frac{\delta g}{g}\right)_i^2\right](\rho g \, \Delta z)_i^2 + \mu_g \left(\frac{\delta g}{g}\right)^2 \sum_i^k \sum_j^k (\rho g \, \Delta z)_i (\rho g \, \Delta z)_j\right]\right\} \qquad (i \neq j)$$

where $0 \leq \mu_g \leq 1$ according to the nonindependence of the error in g with altitude. The assumption here of point-to-point independence in other quantities such as C_D is undoubtedly pessimistic in $\delta T/T$. Further investigation and experience with the passive-sphere technique will provide quantitative information concerning independence and correlation in such quantities.

ACCELERATION AND VELOCITY UNCERTAINTY

Uncertainty in the measured acceleration and velocity of a passive sphere is determined by the accuracy of the tracking instrument and by the length of the data-smoothing interval used in computing time derivatives. (We make the tacit assumption that no error is introduced by the smoothing model, which is tantamount to assuming that the sphere trajectory is exactly of the order or form of the polynomial or other function used in fitting the data.) Bases for a general quantitative evaluation of derivative uncertainty from position uncertainty and smoothing interval length are presented herein.

The tracking system measures the position of the sphere to within some volume of uncertainty which, in turn, may vary in size and shape according to sphere position. The dimension of interest in this volume is that along the drag vector, which for the high altitudes under discussion is parallel to the path tangent. By assuming that the tracking system measures sphere position in slant range R, azimuth angle A, and elevation angle E, with uncertainty in each, δR, δA, and δE, the position uncertainty along the path tangent is given by

$$(\delta X)^2 = \left[\frac{(\dot{R}\delta R)^2 + \left(R^2\dot{E}\delta E\right)^2 + \left(R^2\dot{A}\delta A \cos E\right)^2}{V^2} \right]$$

where

$$V^2 = (\dot{R})^2 + (R\dot{E})^2 + (R\dot{A} \cos E)^2$$

Smoothing of data rests on available discriminating knowledge of the signal and noise in the data. The major characteristic of the signal, which immediately suggests itself, is sphere inertia, which implies a cutoff frequency in sphere velocity response.

Linearizing the drag acceleration about a point on the trajectory provides an expression for the local frequency response.

$$\omega_s = \frac{\rho C_D V}{(m/A)}$$

The corresponding minimum altitude wavelength of density structure to which the sphere can respond is

$$Z_s = \frac{2\pi\dot{z}}{\omega_s}$$

166

The radius Δz of the altitude neighborhood within which a constant ω_S is valid is given by

$$\frac{1}{\omega_S}\left(\frac{\partial \omega_S}{\partial z}\,\Delta z\right) = \left(\frac{1}{\rho}\frac{\partial \rho}{\partial z} + \frac{1}{C_D}\frac{\partial C_D}{\partial z} + \frac{1}{V}\frac{\partial V}{\partial z}\right)\Delta z$$

The first term in the sum is the reciprocal of the local scale height

$$H = \frac{R^* T}{M_W g}$$

the second is small, and the third is proportional to density according to

$$\frac{1}{V}\frac{\partial V}{\partial z} = \frac{\rho C_D}{2(m/A)}\frac{V}{\dot{z}}$$

The first term dominates at high altitude. By assigning a "validity limit" $\Delta\omega_S/\omega_S$, the altitude interval over which constant ω_S holds is $\pm\Delta z = 2H\left(\frac{\Delta\omega_S}{\omega_S}\right)$. The character of low-order polynomial smoothing routines in the frequency domain is approximated by that of a low-pass filter with cutoff frequency ω_f inversely proportional to smoothing interval W.

$$\omega_f = \frac{\pi}{W}$$

The altitude interval traversed during a "window" time length W is proportional to vertical velocity $\dot{z}$, and the minimum altitude wavelength in density structure passed by such a filter is about twice that interval.

$$Z_f = 2W\dot{z} = \frac{2\pi\dot{z}}{\omega_f}$$

Processing the data with a low-pass filter having a cutoff frequency $\omega_f = \omega_S$ would reject considerable noise without disturbing the signal. As altitude increases, however, $Z_S/2$ exceeds its range of validity $2H(\Delta\omega_S/\omega_S)$. Though approaches are conceivable, by using advanced processing techniques which may effectively enable the use of greater smoothing intervals without exceeding the validity of the associated smoothing model, smoothing intervals are currently limited for practical purposes to those over which ω_S is constant, i.e., to $Z_S/2$ or $2H(\Delta\omega_S/\omega_S)$, whichever is smaller.

Matching W to the frequency response of the sphere but limiting it to $2H(\Delta\omega_S/\omega_S)$ requires

$$W = \frac{\pi(m/A)}{\rho C_D V} \qquad\qquad \left[Z_S \leqq 4H(\Delta\omega_S/\omega_S)\right]$$

$$W = \frac{2H}{\dot{z}} \qquad\qquad \left[Z_S > 4H(\Delta\omega_S/\omega_S)\right]$$

For the higher altitudes of interest, the window will depend on H, and therefore, the data are filtered less and less with increasing altitude, relative to sphere response. A variable smoothing interval of this maximum length approximates best that can be done with the standard smoothing techniques of low-order polynomial fitting.

Other noise and signal characteristics which permit the identification of certain desired or undesired components in the data sometimes exist. Special techniques designed for specific components are assumed operative in the present discussion to the extent that their respective net noise components do not exceed the assumed measurement uncertainties.

Time derivatives from a low-pass filter are bounded by the cutoff frequency and by input amplitude. If input uncertainty is δX, then uncertainties in the first and second derivatives are approximated by

$$\delta \dot{X} = \omega_f \delta X$$

$$\delta \ddot{X} = \omega_f^2 \delta X$$

The above relations combine and reduce to an error model for the passive-sphere system at high altitudes. By letting $\dfrac{\Delta \omega_s}{\omega_s} = 1$,

$$\frac{\delta \rho}{\rho} = \left\{ 4\left(\frac{\omega_f \delta X}{V}\right)^2 \left[\left(\frac{\omega_f}{\omega_s}\right)^2 + 4\right] + \left(\frac{\delta C_D A}{C_D A}\right)^2 + \left(\frac{\delta g_V}{g_V}\right)^2 + \left(\frac{\delta m}{m}\right)^2 \right\}^{1/2}$$

The first term is

$$20\left[\frac{\rho C_D}{(m/A)} - \delta X\right]^2 \qquad\qquad \left(Z_f = Z_s\right)$$

$$\left(\frac{\pi}{H}\frac{\dot{z}}{V}\delta X\right)^2 \left[\left(\frac{\pi(m/A)}{2H\rho C_D}\frac{\dot{z}}{V}\right)^2 + 4\right] \qquad\qquad \left(Z_f = 4H\right)$$

A quantitative illustration of this error model, including the associated temperature uncertainty is presented in tables I and II and figure 1.

For reference, a simulated 160-km trajectory in the U.S. Standard Atmosphere 1962 of a 1-meter, 100-gram sphere is used. Arbitrary values for input uncertainties are based on published experience (refs. 1, 2, and 3).

Uncertainty is taken here to correspond to practical limits of error. Uncertainty of the value of a normally distributed random variable is taken as two standard deviations

168

and that of a uniformly distributed quantity its semirange (radius). Quoted uncertainty values for drag coefficient, for example, are understood to mean the limit within which the true value lies with a high (80- to 90-percent) probability. Inputs and results here may be halved throughout to correspond to the standard deviation.

The uncertainty inputs are as follows:

$$\delta R = 9.0 \text{ meters}$$

$$\delta E = \delta A = 0.0001 \text{ radian}$$

$$\frac{\delta C_D A}{C_D A} = 0.03$$

$$\frac{\delta g_V}{g_V} = 0.01$$

$$\frac{\delta m}{m} = 0.01$$

$$\frac{\delta M_W}{M_W} = 0.03$$

OBSERVATION

The quantitative results of the illustration suggest a significant finding concerning the passive-sphere technique. Deviations between sphere results and results from other atmospheric sounding techniques may be explained in large part as a consequence of the smoothing interval used.

It is recommended that data reduction programs include the automatic calculation of the point-to-point uncertainty and present a measured parameter q from a given sounding in the form of q ± Δq, rather than simply as q. Thus, for example, the density profile plot would be a curve with varying width within which the measured density lies with a stated probability. Comparisons between techniques would then be expected to produce overlapping curves.

It is expected that tracking accuracy, δR, δE, δA, will not increase significantly over the assumed values for altitudes considerably higher than 90 km. Therefore, larger data-smoothing intervals would materially enhance the altitude capability of the passive-sphere technique. By assuming successful higher order smoothing models, an upper bound or the maximum possible smoothing interval at a given altitude is the period of the entire trajectory above that altitude including both upleg and downleg portions. Further investigation of the practical capabilities of potential and advanced data processing methods is indicated. The tracking accuracy requirements for a new passive-sphere system must depend on properties of the smoothing interval to be used.

APPENDIX

SYMBOLS

A   sphere cross-sectional area, m^2; radar azimuth angle, radians

a_D drag acceleration, m/sec^2

a_V inertial acceleration along the trajectory, m/sec^2

C_D drag coefficients

E   radar elevation angle, radians or degrees

g   gravity, m/sec^2

g_V gravitational acceleration along the trajectory, m/sec^2

H   atmospheric scale height, m

M   Mach number

M_W mean molecular weight

m   sphere mass, kg

N_{Re} Reynolds number

R   radar slant range, m

R^* universal gas constant, joules/^oK kg-mol

T   atmospheric temperature, ^oK

t   time

V   air speed, m/sec

W   smoothing interval, sec

X   position along trajectory, m

Z_f, Z_s minimum altitude wavelength; passed by smoothing or sensed by
              sphere, respectively, m

z   altitude, m

δq uncertainty along trajectory of any parameter   q

μ_g degree of nonindependence of gravity error with altitude

ρ atmospheric density, kg/m^3

ψ trajectory angle from horizontal, degrees

ω_f, ω_s cutoff frequency of smoothing response or of sphere response, respectively,
              radians/sec

Subscripts:

i,j,k   indices

o   initial

    Dots over a symbol indicate the degree of the derivative with respect to time.

REFERENCES

1. Engler, Nicholas A.: Development of Methods To Determine Winds, Density, Pressure,
    and Temperature From the ROBIN Falling Balloon. AFCRL-65-448, U.S. Air
    Force, May 1965. (Available from DDC as AD630200.)

2. Peterson, J. W.; Hansen, W. H.; McWatters, K. D.; and Bonfanti, G.: Atmospheric
    Measurements Over Kwajalein Using Falling Spheres. NASA CR-218, 1965.

3. Smith, Lawrence B.: Observations of Atmospheric Density, Temperature, and Winds
    Over Kauai. SC-RR-68-523, Sandia Lab., Aug. 1969.

TABLE I

DOWNLEG

t, sec	z, km	V, m/sec	ψ, degrees	R, km	E, degrees	$\dot{R}$, m/sec	$R\dot{E}$, m/sec	$\dot{z}$, m/sec
220	115	960	-72.8	143.9	53.0	-562	-779	-917
225	110	1004	-73.3	140.9	51.3	-575	-821	-963
230	105	1043	-74.2	138.0	49.6	-583	-856	-1004
235	100	1074	-74.8	135.1	47.8	-582	-911	-1037
240	95	1089	-75.9	132.4	45.4	-569	-925	-1055
245	90	1073	-75.7	129.7	43.9	-539	-930	-1042
250	85	986	-76.9	127.2	42.0	-475	-862	-960
255	80	774	-77.4	124.8	39.5	-358	-718	-756
264	75	458	-79.2	122.4	37.8	-208	-406	-450
279	70	254	-83.0	120.1	35.7	-123	-221	-252

z, km	M	N_{Re}	C_D	a_D, m/sec^2
115	2.75	2.41	2.44	0.413
110	3.12	5.99	2.37	.914
105	3.40	14.5	2.20	1.98
100	3.69	38.4	1.84	4.13
95	3.88	101.0	1.51	8.52
90	3.98	277.0	1.29	18.4
85	3.66	645.0	1.19	36.1
80	2.87	1277.0	1.12	53.1
75	1.61	1491.0	1.03	36.8
70	.854	1540.0	.604	13.3

z, km	$\dfrac{\delta\rho}{\rho}$	$\dfrac{\delta T}{T}$	δT, °K	δX, m	$\dfrac{\delta a_D}{a_D}$	$2\dfrac{\delta V}{V}$	Z_f, km	Z_s, km	W, sec
115	0.758	0.909	275.0	12.8	0.757	0.004	36.9	6.+6	20.1
110	.520	.593	153.0	12.6	.519	.005	31.2	3.+6	16.3
105	.314	.349	81.6	12.5	.313	.005	28.4	1.+6	14.1
100	.199	.214	45.0	12.4	.197	.006	25.4	847	12.2
95	.117	.126	24.0	12.2	.113	.006	23.6	424	12.8
90	.067	.076	13.7	12.1	.059	.007	21.8	191	10.5
85	.041	.052	9.4	12.0	.025	.007	21.8	82.4	11.5
80	.034	.046	8.3	11.8	.011	.007	21.7	34.6	14.3
75	.033	.046	9.2	11.7	.008	.008	24.0	17.6	19.2
70	.034	.046	10.1	11.4	.009	.009	26.3	15.1	30.0

TABLE II

UPLEG

t, sec	z, km	V, m/sec	ψ, degrees	R, km	E, degrees	$\dot{R}$, m/sec	$R\dot{E}$, m/sec	$\dot{z}$, m/sec
23.6	115	962	72.8	119.0	75.0	961.7	-35.9	919
18.4	110	1012	73.8	113.9	75.0	1012.0	-24.7	972
13.4	105	1065	74.4	108.7	75.1	1065.0	-13.8	1026
8.6	100	1124	74.9	103.5	75.1	1124.0	-2.32	1085
4.1	95	1197	75.5	98.2	75.2	1197.0	8.93	1159
0	90	1304	76.0	93.1	75.2	1303.0	20.6	1265

z, km	M	N_{Re}	C_D	a_D, m/sec^2
115	2.76	2.40	2.44	0.414
110	3.15	6.04	2.37	.930
105	3.47	14.8	2.19	.413
100	3.87	40.5	1.82	.442
95	4.27	112.0	1.48	10.2
90	4.84	340.0	1.27	26.8

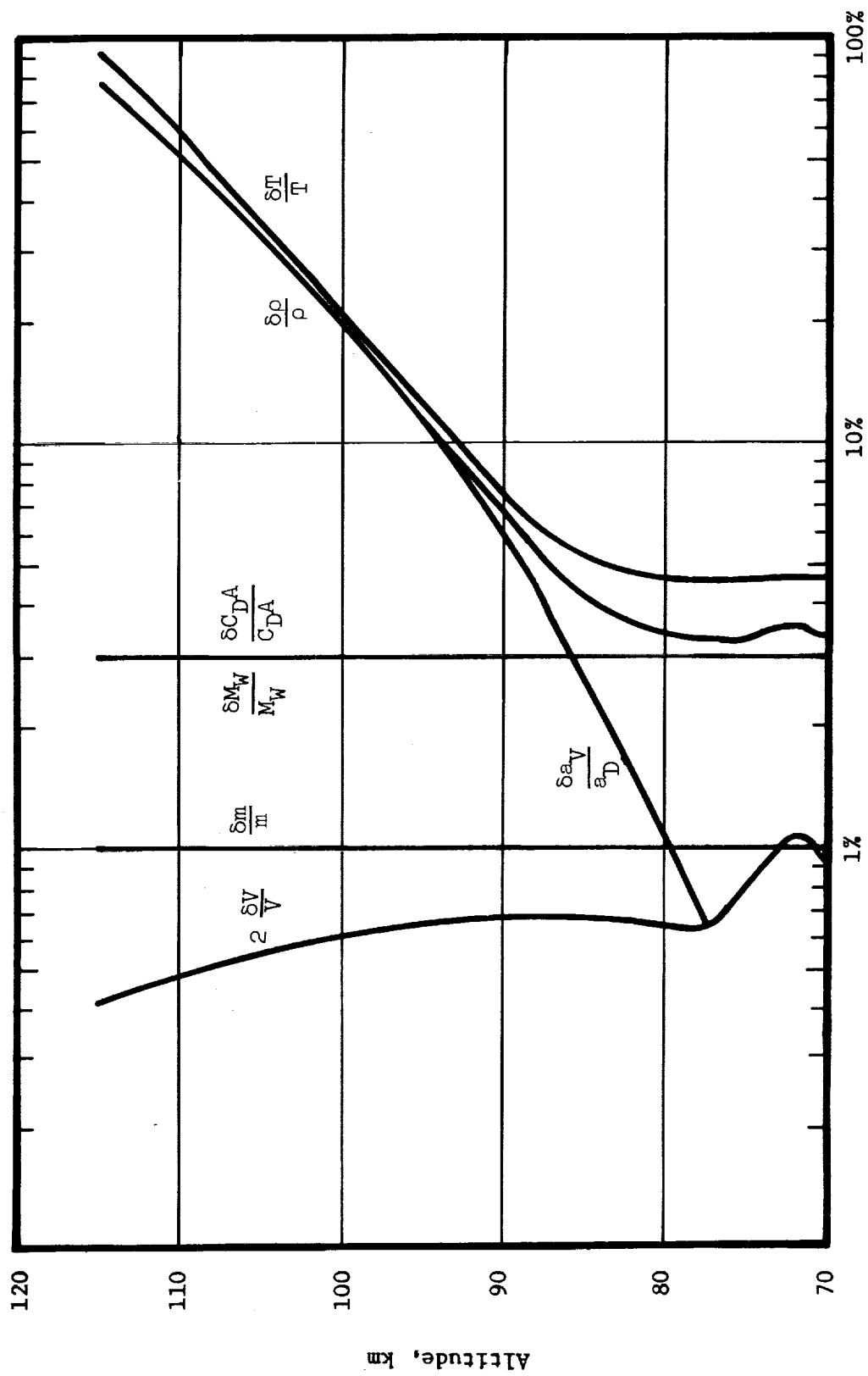| z, km	$\dfrac{\delta\rho}{\rho}$	$\dfrac{\delta T}{T}$	δT, °K	δX, m	$\dfrac{\delta a_D}{a_D}$	$2\dfrac{\delta V}{V}$	Z_f, km	Z_s, km	W, sec
115	0.535	0.735	223.0	9.00	0.534	0.003	36.9	6.+6	2.04
110	.371	.468	120.0	9.00	.369	.003	31.3	3.+6	16.1
105	.228	.273	63.9	9.00	.226	.004	28.4	1.+6	13.9
100	.148	.166	34.9	9.00	.144	.004	25.4	8.+5	11.7
95	.090	.100	19.6	9.00	.084	.005	23.6	427	10.2
90	.055	.065	11.7	9.00	.045	.005	21.8	193	8.6

Figure 1.— Uncertainty components and resultants.

174